DEVELOPMENT AND CALIBRATION OF A WIRELESS, INERTIAL MEASUREMENT UNIT (KLI-PI) FOR RAILWAY AND TRANSPORTATION APPLICATIONS

A BROEKMAN and PJ GRÄBE

University of Pretoria, Engineering 1
University road, Pretoria, 0083
Tel: 012 420 4723; Email: Hannes.Grabe@up.ac.za
Tel: 012 420 4723; Email: andre@broekmail.com

ABSTRACT

With the dawn of the fourth industrial revolution characterized by the rapid advancement and development of 3D printing technologies, miniaturization of transducers and the emergence of big data applications, the railway industry stands to benefit from the implementation of these technologies in the immediate future. "Kli-Pi" is a demonstrative prototype instrument, incorporating a number of these recent advancements in the form of a 9 DoF (Degree of Freedom) IMU (tri-axis accelerometer, gyroscope and magnetometer inertial measurement unit) that can be applied as either an intelligent ballast particle embedded in a railway track, or can be fixed to a particular component under study to measure various response parameters (linear acceleration and angular velocity), recording up to 3,000 data samples per second. The development of both the instrument and its accompanying 3D printed exoskeleton (or shell) is discussed, together with a brief overview of preliminary field testing and its results.

1. INTRODUCTION

Transducers and instrumentation systems, data acquisition and processing technologies and the potential impact of these technologies, are opening up new avenues for the railway engineering sector. To quote Dr. Cheryl Martin's closing remarks from the IHHA 2017 conference: "*The question is what the potential will be for the rail industry. It is no longer a question of whether there will be disruption in the industry, but the question is when it will take place and what the impact will be. There will be changes to what is being moved and who moves it*". Departing from this point, the research topic is postulated: "Development and Calibration of a Wireless, 9 Degree of Freedom, Discrete Element Monitoring Inertial Measurement Unit (Kli-Pi) for Railway Applications." – Rather, the *how, why, when* and *where*, is discussed, in context of current technological trends, products and technologies that can be incorporated in addition to the innovative future research projects that are intended to be undertaken in the near future with the implementation of such an instrument.

2. BACKGROUND

There exists little doubt as to the profound progress made in the miniaturization of semi-conductors and its far reaching effects in the engineering discipline (Spencer et al., 2015). The railway industry has been an early adopter of new, emerging and established technologies to enable and enhance increasingly safer, economical and efficient railway operations especially with regard to both detection and measurement instrumentation (Kouroussis et al., 2015). Selected examples of research applications involving smart sensor platforms and smart ballast in the railway industry are now discussed.

2.1. Smart Sensor Platforms

Klar et al. (2016) defines "smart infrastructure" as: "*an emerging field of study dealing with the development and large-scale embedment of hi-tech sensors in traditional civil engineering structures, and concurrently, with the collecting and meaningful interpretation of raw signals"*. Two complementary, parallel focus areas co-exist to extract valuable information from these networks. First are the consistent performance improvements in processing capabilities, transducers and power delivery-management systems of sensor platforms. Second is the emergence of big data processing, machine learning, data mining and artificial intelligence applications to extract meaningful, accurate and reliable information from these connected systems-of-systems. Recent publications illustrate these constructs that are finding its way into research applications and commercial products and services. Ding (2016) illustrated the use of a Wireless Smart Sensor Node (WSSD) for a wireless, cost effective system for fatigue assessment of rail welds. The system greatly reduces the associated cost of wiring the system to the backbone of a network and is able to be moved and fixed to any point of interest, reducing the number of units that need to be acquired as part of the maintenance program. It is thus not surprising to observe a number of contemporary technologies and instruments being developed and deployed on an extensive scale, with the core-focus shifting to scalable Internet of Things (IoT) technologies to develop interconnected "smart infrastructure" networks.

As noted by Radaj (1996), welded joints are more prone to fatigue and subsequent failure due to pores, inclusions, undercuts and deformation. Such failures can lead to rail breaks and costly derailments, hence the need for easy and cost effective monitoring policies. The wireless sensor node from Ding differs from previous studies in that a high-performance processor, larger memory storage, wireless communication systems, signal conditioners and analog-to-digital converters (ADC) are all integrated in a small, power efficient form factor, known as the Imote2 (Crossbow, 2007). This device can accurately record strain measurements and transmit the data via a standardized 2.4 GHz link for post-processing. The use of these devices extends further than simply analysing a limited set of data. Wessels & Steyn (2016) investigated the use of data obtained from a GPS (Global Positioning System), accelerometers and gyroscopes that are incorporated into anti-theft devices fitted to motor vehicles throughout Southern Africa. Excellent correlation was illustrated between the sensor data and road condition using an equivalent riding quality metric, which can be related to structural and surface deficiencies through the response of the vehicle-road interaction.

2.2. Emergence of Smart Ballast

Zhai et al. (2004) accurately modelled the measured ballast particle accelerations in a ballasted railway track using a uniaxial piezo-electric accelerometer. Dominant frequency spectra in the mid-range of 70 - 110 Hz were recorded. Aikawa (2009) improved this approach by instrumenting a ballast particle with two independent, tri-axial acceleration transducers through which the rotational acceleration can also be derived. Sampling rates of up to 1 kHz were realized which extended the observed frequencies of the ballast to the 350 -500 Hz range. These high frequencies were however damped rapidly together with the ballast particle's rotational movement.

Liu et al.'s (2015, 2016a, 2016b & 2016c) work illustrate the wireless "smart ballast" or "SmartRock" concept as a physical instrument. Published results indicate a correlation between peak angular and peak linear acceleration compared to Discrete Element Models (DEM). Large variations or distributions of the dynamic response of the SmartRock particle situated in the ballast layer are reflected by their model. Making use of 3D printing - an additive manufacturing technology - a robust, protective exoskeleton (shell) was printed to protect the sensitive electronics against damage and attrition. No further information for SmartRock relating to the following performance characteristics is discussed:

- Operational battery life.
- Range and reliability of the data connection in the presence of a noisy electromagnetic environment.
- Strength and durability of the 3D printed shell.
- Range of sampling rates.
- Accuracy, reliability of the chosen IMU chip.

To date, the testing of SmartRock has been limited to laboratory conditions. From the author's viewpoint, the main limitation is the 64 sample per second data transmission rate. Existing studies have proven that a much higher sampling rate is required if ballast resonant frequencies are to be accurately represented and recorded for field testing (Zhai et al., 2004 & Milne et al. 2016). The higher sampling rate also substantially reduces the error associated with integration procedures of acceleration data to obtain displacements (Lamas-Lopez, 2017). From a safety standpoint, the proposed smart ballast unit should be self-sufficient while allowing remote data acquisition and access.

3. KLI-PI DEVELOPMENT

The name “Kli-Pi” is derived from the Afrikaans word for “small rock”; conveying the key notion of a device shaped in the form of a small rock or ballast particle. Kli-Pi is comprised of two main components: a stand-alone internal unit containing all the necessary electronics for the IMU and the 3D printed external exoskeleton or shell, which can be easily joined into place to protect the IMU when embedded in geotechnical or railway structures subjected to large forces (Figure 1).

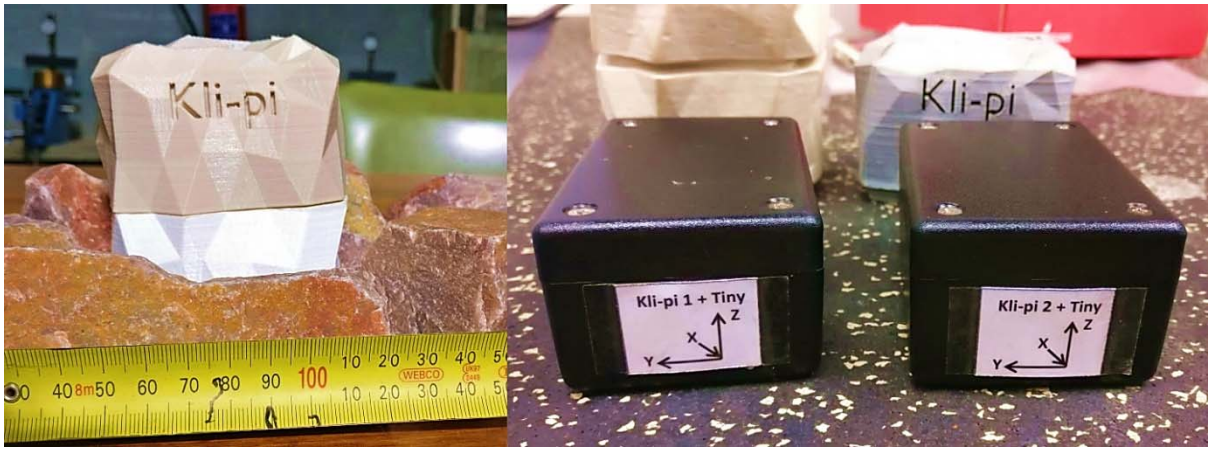

Figure 1: Kli-Pi 3D printed shell / exoskeleton and the internal IMU box containing all the electronics

3.1. Internal IMU

The specifications and properties of the internal unit is summarised:

- A 3 mm thick, IP54 rated, ABS box measuring 40 x 56 x 81 mm in size encapsulating all the electronics.
- The 9 DoF (tri-axial accelerometer, gyroscope and magnetometer) MEMS (Micro-Electro-Mechanical Sensor) IMU IC (Integrated Circuit), measuring only 4 x 4 x 1 mm in size.
- The IMU is connected to and controlled by a high-performance micro-processor that can permanently store the data on a MicroSD card.
- Wireless communication over a high-bandwidth Wi-Fi connection through the operating system (OS) allows the device to function as an IoT device.
- The device contains a rechargeable Lithium-Ion battery that can be recharged using an inductive coupling emitter-receiver unit that allows for complete wireless operation.
- With the current configuration, a continuous data stream comprised of 3,000 samples per second can be stored for a maximum duration of 10 hours on a full battery charge.
- The stand-by time is extended to 2 months with the addition of a second, independent micro-controller in the same IMU unit.
- The IMU chip is fitted with a fabricated heatsink and adapter to minimize temperature fluctuations and high-frequency thermal variance.
- The sampling rate and full scale (FS) can be configured to the user’s requirements.

The unit was stress-tested at an acceleration of 50 G for 1 hour in a geotechnical centrifuge (Jacobsz et al., 2014) whereby uninterrupted, real-time communication remained viable throughout the test. Table 1 summarizes the full scale and maximum sampling rate (per axis) for each sensor on the IMU IC. Sufficient full scale and sampling capabilities provide flexibility for measuring both small and large amplitude signals over a wide range of frequencies.

Table 1 – Full scale and maximum sampling rate for the 9 DoF IMU

Sensor	Full scale (FS)	Maximum Sampling Rate / Axis
Accelerometer (linear acceleration)	±16 G / ±150 m^2/s	1600 Hz
Gyroscope (angular velocity)	±2000 DPS / ±333 RPM	800 Hz
Magnetometer (magnetic flux)	±12 Gauss / ±1.2 mT	100 Hz

The micro-controller is configured to control the power delivery to the micro-processor using low-Voltage power switch IC's that allows for remote power-state control. The battery and charging circuitry is shared between the micro-processor and micro-controller unit. Both the micro-processor and micro-controller can be configured and controlled remotely using a computer or a mobile smartphone running Android or iOS, allowing for flexible and reliable control in adverse environmental conditions.

3.2. 3D Printed Shell

The protective shell serves as an additional protective layer for the IMU, creating a morphologically compatible ballast particle for integration into a railway track. The shell was designed based on the dimensions of the IMU using Blender, an open-source animation software suite. Using an icosahedron as a starting point, the mesh was iteratively subdivided, followed by suitable vertex placement (convex and non-convex configuration) around the outside of the IMU. This provided an easy procedure to create the required angular shape with sufficient thickness, paying careful attention to corner stress concentrations that can occur. The final design was divided into two halves with an added friction-lock mechanism, allowing for effortless integration with the IMU without additional tools. Logos and orientation axes were etched rather than painted onto the geometry using Boolean cut operations, to prevent buffing over time. The shell was printed using a RoboBeast 3D printer using standard Polylactic acid (PLA) filament of various colours (Broekman, 2017a). An outer shell thickness of 4 layers was incorporated together with a 50 % triangular infill to provide resistance against punching and yielding respectively (Figure 2). A print layer height of 0.2 mm was used throughout. A unit that was tested under static loading conditions (one half of the shell) corresponded very well to published material models of PLA (Bergstrom et al., 2013), only yielding at an applied axial force of approximately 40 kN. Only localized damage was visible, even for large strains in excess of 10 %. Preliminary durability testing under dynamic loading – 30 ton axles load for 1,500 cycles - indicated no significant damage to either the shell or the IMU box, providing satisfactory performance for research applications; in fact, granitic ballast placed on top of the Kli-Pi unit was pulverized against the face of the shell.

Figure 2: Unfinished shell print illustrating the geometry and internal structure

4. CALIBRATION

Calibration of any instrument is crucial to obtaining both accurate measurements and results. Difficulty arises when using tri-axial IMU's that incorporate three different transducer technologies altogether. As geotechnical and transportation applications are of prime research interest, only the accelerometer and gyroscope were calibrated. Traditionally a secondary, calibrated instrument such as a centrifuge or a vibration table would be required to calibrate the gyroscope and accelerometer respectively. This increases the unit cost and complexity of the instrument substantially. Skog & Händel's (2006) method uses the principle that the norm of the accelerometer and gyroscope vectors is equal to the norm of the applied acceleration and angular velocity respectively. A cost model is constructed (Equation 1), whereby the coefficients are acquired through finding the minimum cost value for all n-sets of measurements (using Newton's Method):

$$L(\theta_a) = \sum_{i=0}^{n-1}(\|\bar{u}^m\|^2 - \|h(\bar{y}^m, \theta)\|^2)^2 \quad (1)$$

Where:

$\bar{u}^m$ – measured mean of the m-th orientation and rotation

$\bar{y}^m$ – sample mean of the m-th orientation and rotation

The 9 unknown coefficients are assigned to the vector θ, representing the non-orthogonality of the accelerometers, bias values and non-uniform scaling factors for all three axes. Fong et al. (2008) improved Skog & Handel's method by allowing for calibration of the gyroscope without a precision controlled turning table or centrifuge. They proposed an orientation integration algorithm, comparing the transducer outputs with that of the accelerometer, for arbitrary motions. A total of 21 unknown parameters are to be solved to fully define all the unknown coefficients of the matrix formulations; 24 rotations defined the coefficients to a sufficiently level of accuracy. Solving for the unknown coefficients by means of minimizing the cost function is accomplished using a Python script, requiring less than 5 minutes on a standard quad-core processor laptop computer to solve.

5. RESULTS AND DISCUSSION

For the initial calibration of the gyroscope, to validate the proposed calibration procedure, a digitally controlled lathe (HAAS TL-1) was utilized to rotate the IMU at various, constant angular velocities (Broekman, 2017b). Table 2 and Table 3 summarize the statistics that quantify the performance after the calibration procedure for both the accelerometer and gyroscope respectively, indicating the advantage of using the calibration procedure as discussed. The mean value of the measured gravitational acceleration moves closer to unity with smaller deviations for increased accuracy. The accuracy of the gyroscope is also improved with the scale factors requiring adjustment of up to 10 %. The measured linear and angular accelerations proved sufficiently large, with a signal-to-noise ratio for vertical accelerations exceeding 100. The calibration factors are applied during the post-processing phase of the data analysis.

Table 2: Calibrated parameters for Kli-Pi tri-axis accelerometer (average of 50 static measurements)

Parameter	Uncalibrated (G)	Calibrated (G)	% Improvement
Minimum Value	0.936	0.997	N/A
Maximum Value	1.049	1.018	N/A
Mean	0.989	1.004	N/A
Accuracy	±0.049	±0.018	63
Standard Deviation	0.036	0.005	87

Table 3: Calibrated parameters for Kli-Pi tri-axis gyroscope (average of dynamic measurements)

Parameter	Uncalibrated (RPM)	Calibrated (RPM)	% Improvement
Accuracy (X)	±5.959	±1.781	70
Accuracy (Y)	±4.118	±2.699	34
Accuracy (Z)	±4.103	±3.441	16

The first Kli-Pi prototype was tested during March 2017 near Vryheid on Transnet's Heavy Haul Coal Line, situated in the Kwa-Zulu Natal province of South Africa. The site is located near a tunnel entrance where large displacements were observed near the transition zone. The IMU unit was positioned on top of the crib ballast, sleepers and the web of the rail. For all cases good sensitivity was observed, particularly for the small displacements from the ballast (smaller than 400 μm), and rotation of the rail (0.15 degrees). Notably, enthralling behaviour was observed for longitudinal (x-axis), lateral (y-axis) and vertical displacement (z-axis) when the IMU was attached to the web of the rail (Figure 3). In the longitudinal direction, the tractive forces of the locomotives are apparent. The lateral and vertical displacements measure near equal displacements at selected points in time, despite the different moments of inertia of the rail about the respective axes.

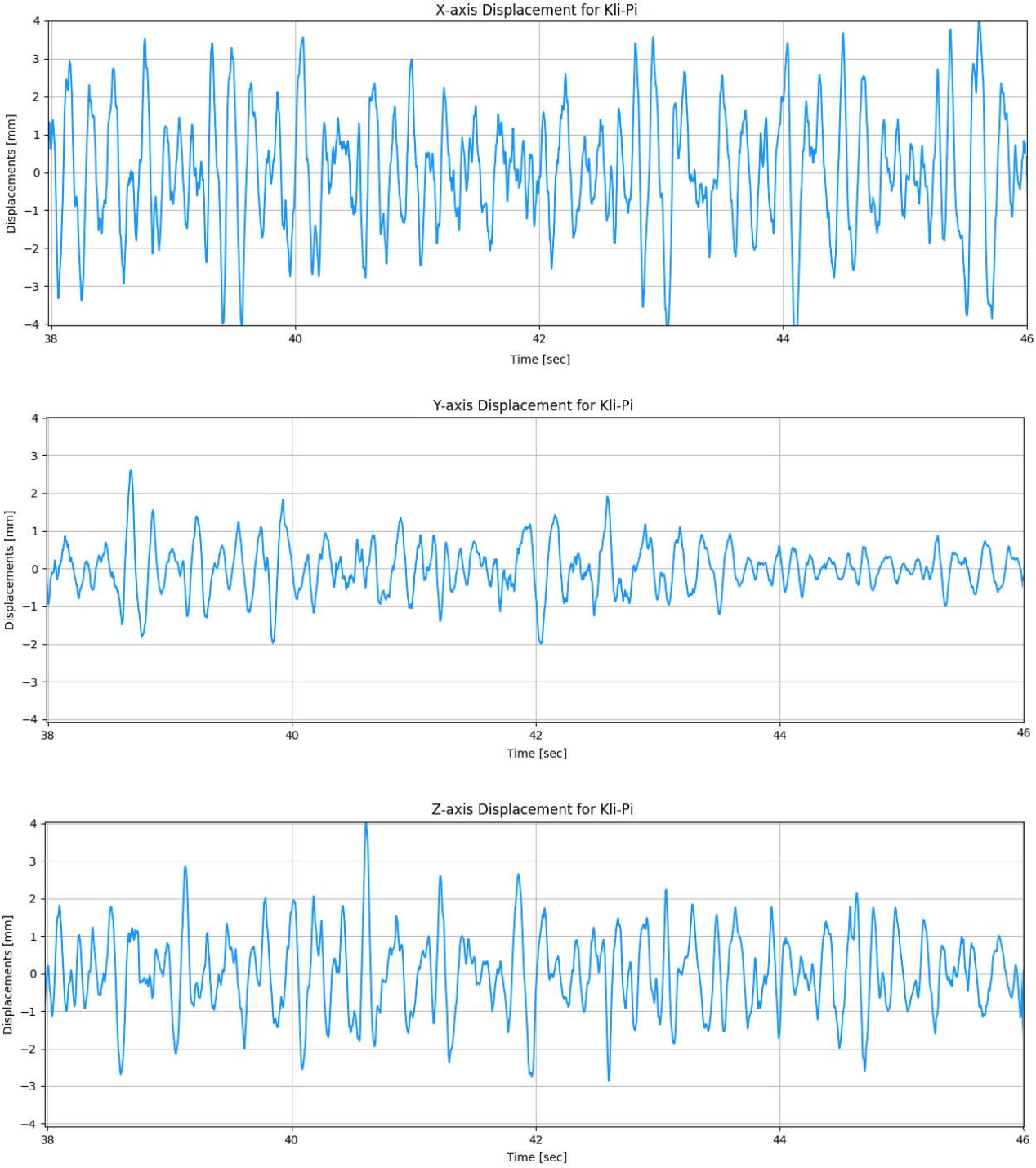

Figure 3: Displacement in three dimensions for both locomotives and wagons

Figure 4 illustrates the different in-plane rotations for both the locomotives and the trailing wagons. A clear correlation between the in-plane displacement and rotation of the rail is visible when superimposing the measurements (Broekman, 2017c).

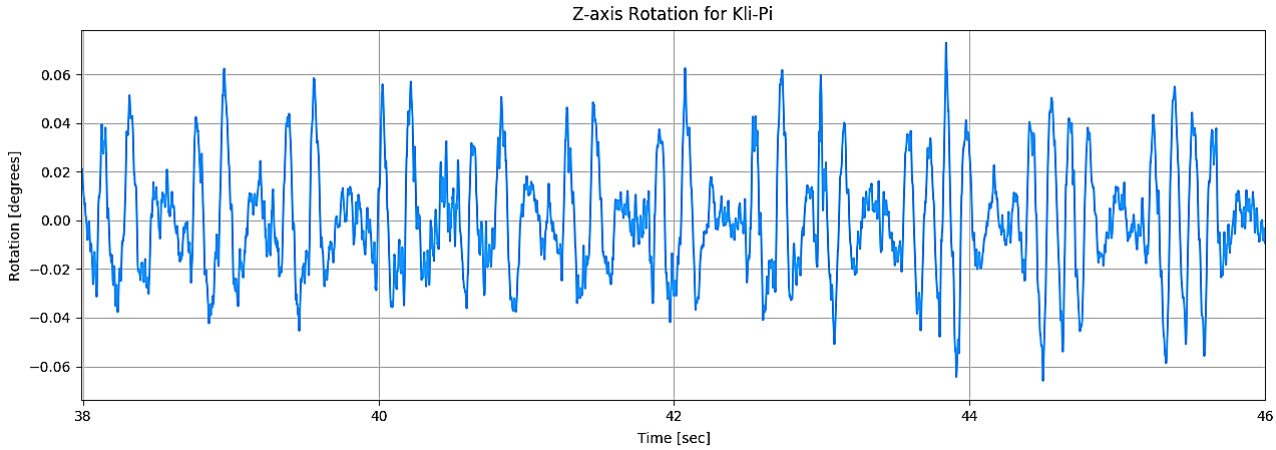

Figure 4: In-plane rotations for both locomotives and wagons

6. CONCLUSIONS & RECOMMENDATIONS

"Kli-Pi" as it is known, promises to be a valuable and nimble instrument for augmenting new and existing research activities in the railway and other transportation fields, given the small, high-performance specifications. As stated, the emergence of smart infrastructure requires dedicated planning, development and experimentation to realize the potential of new technologies and information services associated with the fourth industrial revolution. This continuing research project serves as a proof-of-concept and testing ground for these new technologies. Preliminary testing presents the capability for applying low-cost, miniaturized MEMS transducers to obtain accurate and high-density data measurements that would otherwise be impossible using traditional methods. Prospective future research applications include investigating in-situ ballast displacement and rotations in three dimensions, studying the dynamic ballast response of transition zones, wheel-rail interaction by fixing the IMU to the locomotive or wagon wheels and addressing fixity and continuity uncertainties of ballastless track technologies.

7. ACKNOWLEDGEMENTS

The University of Pretoria, the laboratory staff and lecturers of the Department of Civil Engineering are acknowledged for supporting the project and providing valuable insight and recommendations during the development and testing phase of Kli-Pi. MakerSpace coordinator, Sean Kruger, for the assistance and availability of the MakerBot and RoboBeast 3D printers. Transnet Freight Rail is thanked for sponsoring the Chair in Railway Engineering at the University of Pretoria.

8. REFERENCES

Aikawa, A, 2009. Techniques to Measure Effects of Passing Trains on Dynamic Pressure Applied to Sleeper Bottoms and Dynamic Behaviour of Ballast Stones. Quarterly Report of the Railway Technical Research Institute of Japan, Volume 50, No. 2, Japan.

Bergstrom, J, Quinn, D, Chow, S & Govindarajan, S, 2013. Non-linear Viscoplastic Material Modeling of the Degradation Response of PLA. Proceedings of the ASME 2013 Conference on Frontiers in Medical Devices: Applications of Computer Modeling and Simulation, 11-13 September, Washington, DC, USA.

Broekman, A, 2017a. 3D MakerBot printing at UP's Makerspace. Available at: https://youtu.be/v0HNlNEXvpA (Accessed: 12 January 2018)

Broekman, A, 2017b. Kli-Pi Calibration procedure comparison using a lathe. Available at: https://youtu.be/mX1rKXyPEjQ (Accessed: 12 January 2018)

Broekman, A, 2017c. Rail movement in 3D (Kli-Pi) – Vryheid, South Africa (2017). Available at: https://youtu.be/KZreWHDqJd4. (Accessed: 12 January 2018)

Cloete, K, 2017. Companies urged to join the digital revolution. Creamer Media's Engineering News. 6 September [Online]. Available at: http://m.engineeringnews.co.za/article/companies-urged-to-join-the-digital-revolution-2017-09-06/rep_id:4433 [Accessed January 12, 2018].

Crossbow Technology, Inc. 2007. Imote2 Hardware Reference Manual. San Jose, CA.

Ding, HP, 2016. Design of a Wireless Smart Sensor Node for Fatigue Assessment of Welded Joints. Proceedings of the International Conference on Smart Infrastructure and Construction, ICE Publishing, United Kingdom, pp 135-141.

Fong, W, Ong, S, & Nee, A, 2007. Methods for In-Field User Calibration of an Inertial Measurement Unit without External Equipment. Measurement Science and Technology, Volume 19, pp 1-11.

Jacobsz, S, Kearsley, E, & Kock, J, 2014. The Geotechnical Centrifuge Facility at the University of Pretoria. Proceedings of the 8th International Conference on Physical Modelling in Geotechnics, 14-17 January, Perth, Australia, pp 169-174.

Klar, A, Levenberg, E, Tur, M, & Zadok, A, 2016. Sensing for Smart Infrastructure: Prospective Engineering Applications. Proceedings of the International Conference on Smart Infrastructure and Construction, 27-29 June, ICE Publishing, United Kingdom, pp 289-295.

Kouroussis, G, Caucheteur, C, Kinet, D, Alexandrou, G, Verlinden, O & Moeyaert, V, 2015. Review of Trackside Monitoring Solutions: From Strain Gauges to Optical Fibre Sensors. Sensors, Volume 15, Issue 8, pp 20115-20139.

Lamas-Lopez, F, Cui, Y.J, Costa Aguiar, S & Calon, N, 2017. Assessment of Integration Methods for Displacement Determination using Field Accelerometer and Geophone Data. Journal of Zhejiang University, Volume 18, Issue 7, pp 553-566.

Liu, S, Huang, H, & Qiu, T, 2015. Laboratory Development and Testing of “SmartRock” for Railroad Ballast using Discrete Element Modeling. Proceedings of the 2015 Joint Rail Conference (JRC2015), March 23–26, San Jose, California, USA.

Liu, S, Huang, H, Qiu, T, Gao, L, 2016a. Comparison of Laboratory Testing Using SmartRock and Discrete Element Modeling of Ballast Particle Movement. Journal of Materials in Civil Engineering, Volume 29, Issue 3.

Liu, S, Qiu, T, Haung, H, & Gao, Y, 2016b. Study on Ballast Particle Movement at Different Locations Beneath Crosstie Using “SmartRock”. Proceedings of the 2016 Joint Rail Conference (JRC2016), April 12-15, Columbia, SC, USA.

Liu, S, Huang, H, Qiu, T, Kwon, J, 2016c. Effect of geogrid on railroad ballast particle movement. Transport Geotechnics.

Milne, D, Le Pen, L, Watson, G, Thompson, D, Powrie, W, Hayward, M & Morley, S, 2016. Measuring Ballast Acceleration at Track Level. Third International Conference on Railway Technology: Research, Development and Maintenance.

Radaj, D, 1996. Review of Fatigue Strength Assessment of Nonwelded and Welded Structures Based on Local Parameters. International Journal of Fatigue, Volume 18, No. 3, pp 153-170.

Skog, I, & Händel, P, 2006. Calibration of a MEMS Inertial Measurement Unit. Proceedings of the 17th IMEKO World Congress, 11-17 September, Rio de Janeiro, Brazil.

Spencer, B.F (Jr), Jo H, Mechitov, K.A, Li J, Sim, S.H, Kim, R.E, Cho, S, Linderman, L.E, Moinzadeh, P, Giles, R.K & Agha, G, 2015. Recent Advances in Wireless Smart Sensors for Multi-scale Monitoring and Control of Civil Infrastructure. Journal of Civil Structural Health Monitoring, Volume 6, pp 17–41.

Smith, C, 2017. Equal distribution of benefits needed - WEF expert. Fin24. 4 September [Online]. Available at: http://www.fin24.com/Economy/equal-distribution-of-benefits-needed-wef-expert-20170904 [Accessed September 16, 2017].

Wessels, I, & Steyn, WJvdM, 2016. Real-time Monitoring of the Extended Road Network by Utilising Telematics Technology. 4th Chinese European Workshop on Functional Pavement Design, Delft, Netherlands, pp 1645-1656.

Zhai, WM, Wang, KY & Lin, JH, 2004. Modelling and experiment of railway ballast vibrations Journal of Sound and Vibration, Volume 270, pp 673–683.